Peremennye Zvezdy (*Variable Stars*) **45**, No. 4, 2025

Received 3 January; accepted 30 January.

DOI: 10.24412/2221-0474-2025-45-45-53

Photometry of the Classical Nova V1112 Per

Igor Volkov

Sternberg Astronomical Institute, Moscow University, Universitetsky Ave., 13, 119992 Moscow, Russia

High precision photometric observations of the bright Nova V1112 Per at early stages after its outburst are presented. We found the time of the star's maximum brightness, estimated its interstellar extinction using empirical formulas. Our data made it possible to determine the mass of white dwarf $M_{\rm wd} = 0.82 \pm 0.07 M_\odot$ and the distance to the star $d = 5.2 \pm 0.4$ kpc. Fast variability at early stages was detected.

1 Introduction

Nova Persei 2020 = V1112 Per = TCP J04291888+4354233 was discovered by Seiji Ueda on 2020 Nov 25.813 UT and classified as a classical nova by Munari et al. (2020). According to the AAVSO light curve, the nova reached its maximum ($V = 8^{\rm m}_{.}24$, $B = 9^{\rm m}_{.}03$, with $B-V = 0^{\rm m}_{.}79$) on JD 2459186.77 and not on JD 2459183.396, as suggested by Chochol et al. (2020): after the proposed date of the outburst, the average brightness of the star definitely increased and reached the absolute maximum on the date we determined, see Fig. 3 below. Our observations started 10 days after the maximum brightness, they include 29 observing nights and cover a time interval of 118 days. The main array of observations was obtained with the 1-m telescope of Simeiz observatory (Institute of Astronomy, Russian Academy of Sciences) in combination with CCD FLI 09000 and Bessel $UBVRcIc$ set of filters (Nikolenko et al. 2019). On five nights, observations were carried out in the $UBVRIRc$ Johnson–Cousins system with the Zeiss-600 telescope of the same observatory using the VersArray 512UV CCD.

2 Observations and reductions

Magnitudes of the brightest star in the field, HD 276383, were obtained by fitting to the star LD 115 420 = GSC 586 717 from Landolt (2009) using the Zeiss-1000 instrumentation. Although the Landolt standard is equatorial and far from the variable star, our altitude-matched calibration proved very accurate and closely aligned with B, V data in Simbad and APASS catalogues. HD 276383 is located only $2'_{.}7$ from the nova and served as a reference star. To study the interstellar absorption in the direction of V1112 Per, magnitudes of stars in its vicinity were measured relative to HD 276383. The results are presented in Table 1 and in Fig. 1. A chart of the area with the numbers of measured stars is shown in Fig. 2. From the two-color diagram in Fig. 1, it is obvious that the region experiences significant interstellar absorption. Magnitudes of HD 276383 in near-infrared bands of the Johnson system can be determined using formulas from Taylor (1986): $R = 8^{\rm m}_{.}577 \pm 0^{\rm m}_{.}009$, $I = 7^{\rm m}_{.}868 \pm 0^{\rm m}_{.}011$.

Table 1: $UBVRcIc$ magnitudes of stars in the field of V1112 Per

Star	U	B	V	Rc	Ic	$U-B$	$B-V$	$V-Rc$	$Rc-Ic$	Remark
1	12.015	10.996	9.717	8.922	8.284	1.019	1.279	0.794	0.638	HD276383
	0.002	0.002	0.002	0.002	0.002	0.003	0.003	0.003	0.003	
3	13.426	13.194	12.422	11.908	11.532	0.232	0.772	0.514	0.376	GSC 2891 2673
	0.010	0.002	0.001	0.001	0.001	0.010	0.002	0.001	0.001	
4	13.590	13.415	12.632	12.109	11.679	0.175	0.783	0.523	0.430	GSC 2891 2701
	0.006	0.015	0.006	0.001	0.001	0.015	0.015	0.006	0.001	
5	13.814	13.638	12.781	12.219	11.736	0.176	0.857	0.562	0.483	GSC 2891 2903
	0.010	0.012	0.004	0.001	0.001	0.012	0.012	0.004	0.001	
6	14.708	13.799	12.434	11.551	10.748	0.909	1.365	0.883	0.803	GSC 2891 2877
	0.049	0.077	0.010	0.001	0.001	0.077	0.077	0.010	0.001	
7	16.140	15.112	13.713	12.855	12.104	1.028	1.399	0.858	0.751	GSC 2891 2511
	0.022	0.032	0.016	0.002	0.002	0.032	0.032	0.016	0.003	
8	15.354	14.974	14.436	14.112	13.817	0.380	0.538	0.324	0.295	
	0.142	0.018	0.007	0.004	0.007	0.142	0.018	0.007	0.008	
9	16.031	15.160	13.649	12.733	11.906	0.871	1.511	0.916	0.827	GSC 2891 2691
	0.211	0.044	0.010	0.001	0.002	0.211	0.044	0.010	0.002	
10	13.321	13.037	12.515	12.185	11.889	0.284	0.522	0.330	0.297	GSC 2891 2677
	0.090	0.016	0.001	0.001	0.001	0.090	0.016	0.001	0.001	
11	15.201	14.761	13.690	12.993	12.396	0.440	1.071	0.697	0.597	
	0.034	0.022	0.003	0.002	0.002	0.034	0.022	0.003	0.003	
12	16.119	14.713	13.300	12.423	11.664	1.406	1.413	0.877	0.759	GSC 2891 2532
	0.310	0.019	0.012	0.001	0.001	0.310	0.019	0.012	0.001	
13	14.495	14.217	13.171	12.496	11.891	0.278	1.047	0.675	0.605	GSC 2891 2469
	0.007	0.002	0.001	0.001	0.002	0.007	0.002	0.001	0.002	
14	15.545	14.675	13.634	12.924	12.407	0.870	1.041	0.710	0.517	GSC 2891 2789
	0.017	0.003	0.002	0.001	0.002	0.017	0.004	0.002	0.002	

Individual $UBVR_cI_cR_JI_J$ measurements of V1112 Per are presented in the electronic appendix to html version of this article as a zip archive. The first column of the tables gives the Julian Heliocentric Date of mid-exposure minus 2400000, the second column is the stellar magnitude of the object.

After the brightness of V1112 Per became lower, the exposures had to be increased and the star No. 4 from Table 1 was used as a reference object.

3 Basic parameters and classification of V1112 Per

The brightness measurements on each of the observing nights were averaged and are given, together with their errors, in Table 2. The corresponding plots are shown in Figs. 3 and 4. For band B, AAVSO measurements are also shown. Comparison of the AAVSO and our graphs shows that the nebular stage of brightness decline occurred around JD 2459270, see Fig. 3. At this point, the B graph definitely splits into two. This bifurcation is due to the fact that instrumental systems of AAVSO observers are slightly different from ours and from each other. Thus, when observing stars with emission spectra, some bright spectral lines may be situated at the edge of a given photometric band. In such a case, differences in measured brightness can exceed one stellar magnitude, as it happened, for example, for the slow Nova V475 Sct, in the spectrum of which at the beginning of the nebular stage, very strong emission [OIII] 495.89 nm and 500.69 nm lines had developed. These lines are located just at the edge of the transmission curves of B and V bands and are

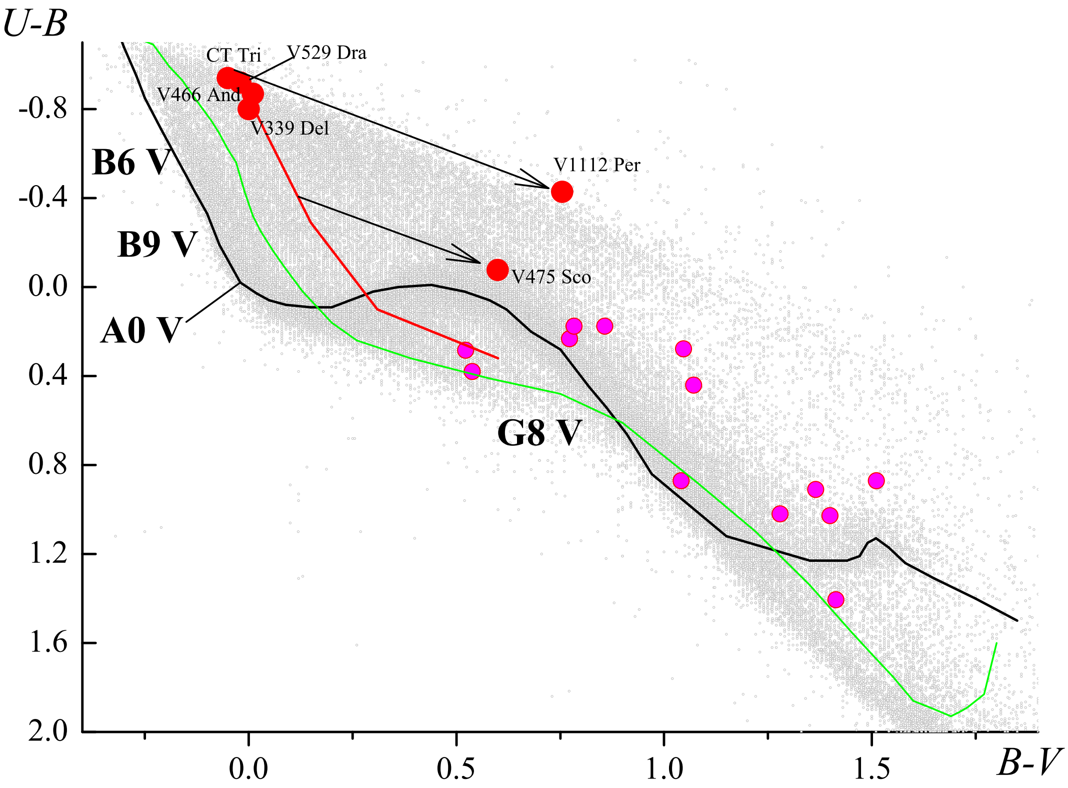

Figure 1.
The $U-B, B-V$ diagram of V1112 Per and field stars. The red broken line is the novae–giant sequence (Hachisu & Kato 2014). The gray background represents data from the Mermilliod et al. (1997) catalogue. Magenta circles represent field and comparison stars. The red circles show positions of several Novae during the expansion stage of the dense shell, including the object under study. Arrows indicate interstellar reddening lines.

responsible for the discrepancy of B and V magnitudes determined from our observations taken with different instruments (Chochol et al. 2005ab).

The V and B light curves and AAVSO data were used to find the decline rates $t_{2,V} = 21$ days, $t_{3,V} = 33.5$ days, $t_{2,B} = 23$ days, $t_{3,B} = 34.5$ days. This means that V1112 Per belongs to slow Eddington novae ($t2 > 13$ days, $t3 > 30$ days), it has a structured light curve with standstill at maximum and dust formation at later stages. It may belong to the Fe II spectroscopic type (Downes & Duerbeck 2000).

One can estimate the absolute magnitudes of V1112 Per at maximum MV_{max}, MB_{max} using the MMRD (Magnitude at Maximum Rate of Decline) relations:

(1) absolutely calibrated $MV_{max} - t_2$ relation (Della Valle & Livio 1995):

$$MV_{max} = -7.92 - 0.81 \arctan \frac{1.32 - \log t_2}{0.23}, \tag{1}$$

$MV_{\rm max} = -7\overset{\rm m}{.}47$.

(2) $MV_{max} - t_2$ relation (Downes & Duerbeck 2000):

$$MV_{max} = (-11.32 \pm 0.44) + (2.55 \pm 0.32) \log t_2, \tag{2}$$

$MV_{\rm max} = -7\overset{\rm m}{.}95$.

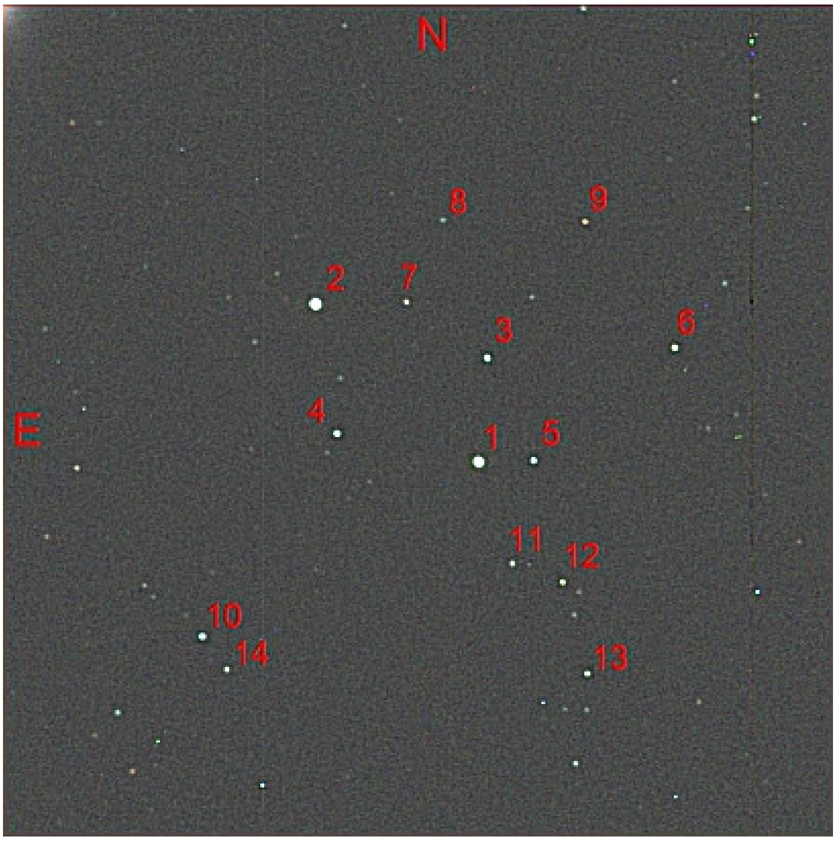

Figure 2.
V1112 Per = No. 2 and local standard stars. The color image was obtained combining $BVIc$ frames from the 1-m telescope. The side of the square is $10'$. Magnitudes of the stars are presented in Table 1.

(3) MV_{15} empirical relation (Downes & Duerbeck 2000). The cited authors found that Novae 15 days after maximum had similar absolute magnitudes $MV15 = -6.05 \pm 0.44$:

$$MV_{15} = -6^{\mathrm{m}}_{.}05 \pm 0^{\mathrm{m}}_{.}44, \tag{3}$$

$MV_{\max} = -7^{\mathrm{m}}_{.}56$.

(4) The $MB_{\max} - t_3$ relations (Pfau 1976; Livio 1992):

$$MB_{\max} = -10.67 \pm 0.30 + (1.80 \pm 0.20) \log t_3, \tag{4}$$

$MB_{\max} = -7^{\mathrm{m}}_{.}90$.

(5) MB_{15} empirical relation (Pfau 1976):

$$MB_{15} = -5.74^m \pm 0.60^m, \tag{5}$$

$MB_{max} = -7^{\mathrm{m}}_{.}09$.

The unweighted mean absolute magnitudes: $MV_{\max} = -7^{\mathrm{m}}_{.}66 \pm 0^{\mathrm{m}}_{.}15$, $MB_{\max} = -7^{\mathrm{m}}_{.}50 \pm 0^{\mathrm{m}}_{.}40$.

The calculated intrinsic color index at maximum light, $(B - V)^{\mathrm{in}}_{\max} = 0.16$, is close enough to that derived by Downes & Duerbeck (2000) for the intrinsic colors of novae at maximum, $(B - V)^{in}_{max} = 0.25 \pm 0.05$, and this implies $MB_{max} = -7^{\mathrm{m}}_{.}41$. Since the accuracy of the maximum brightness estimate in the V band is significantly higher than for the B band, the maximum value in the B band can be accepted as the average of the two estimates, $MB_{\max} = -7^{\mathrm{m}}_{.}45 \pm 0^{\mathrm{m}}_{.}25$.

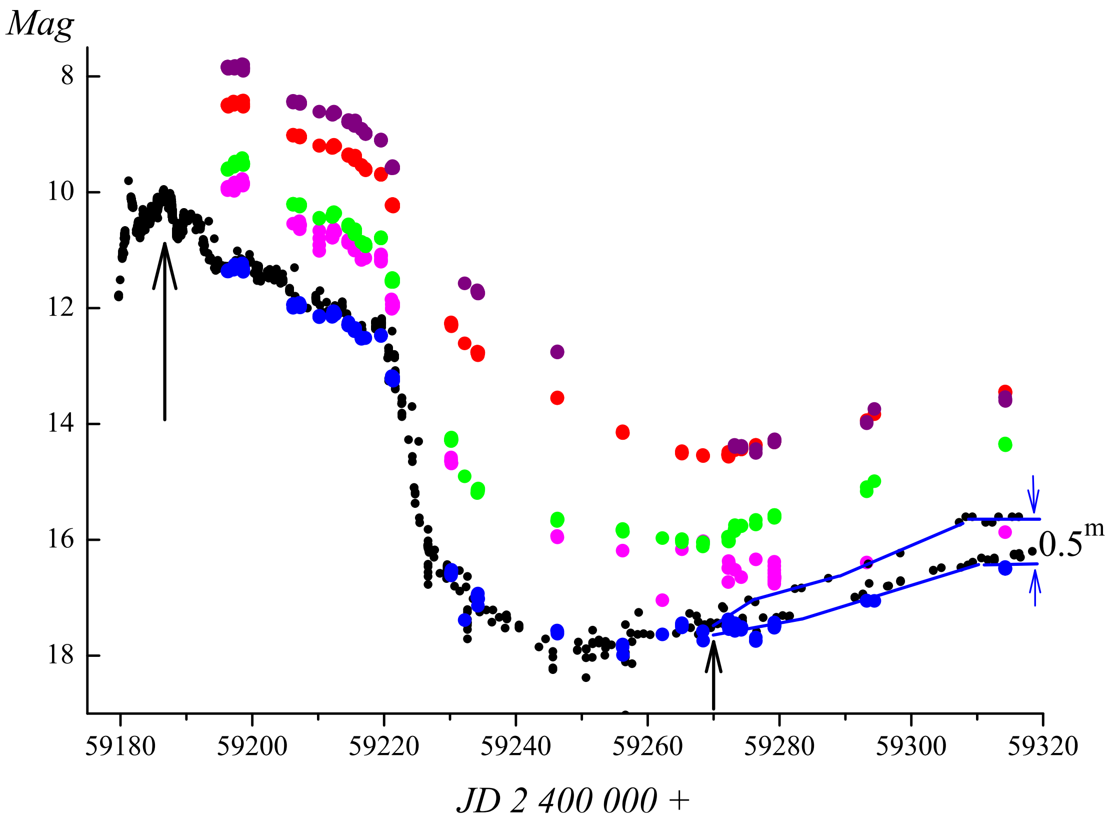

Figure 3.
U, B, V, Rc, Ic light curves of V1112 Per. U – magenta, B – blue, V – green, Rc – red, Ic – brown filled circles. Small black points are AAVSO B data. All B magnitudes were increased by 1^{m}. The first black arrow stays for maximum brightness, the second one marks the beginning of nebular stage. Small arrows indicate the influence of the difference in the instrumental B systems for photometric measurements during the nebular stage.

Using the derived $MB_{\max}$ and the formula given by Livio (1992):

$$MB_{\max} = -8.3 - 10.0\ \log(M_{\mathrm{wd}}/M_{\odot}), \tag{6}$$

we can estimate the mass of the white dwarf in V1112 Per as $M_{\mathrm{wd}} = (0.82 \pm 0.07)M_{\odot}$.

The interstellar extinction of the Nova can be derived:

(1) from the comparison of the observed $B-V$ index at maximum $(B-V)_{\max} = 0\overset{\mathrm{m}}{.}79$, affected by extinction, to the intrinsic color index $MB_{\max} - MV_{\max} = 0\overset{\mathrm{m}}{.}25$, $E(B-V) = 0\overset{\mathrm{m}}{.}54$;

(2) by comparison of the $U-B$ and $B-V$ indices during the opaque shell stage in the $U-B$, $B-V$ diagram to the novae–giant sequence according to Hachisu & Kato (2014). This gives $E(B-V) = 0\overset{\mathrm{m}}{.}79$, see Fig. 1. To demonstrate this method, some other Novae measured by us at the same stages were placed on the $U-B$, $B-V$ diagram, see Fig. 1. The stars CT Tri (Chochol et al. 2009), V529 Dra (Katysheva et al. 2013), V466 And (Chochol et al. 2010) experience little or no absorption, while the star V475 Sco (Chochol et al. 2005b) experiences significant absorption. $E(B-V) = 0.18^{m}$ for V339 Del (Chochol et al. 2014), and it fits better into the supergiant sequence;

(3) from the relation of van den Bergh & Younger (1987), who found that novae two magnitudes below maximum have an unreddened color index

$$B - V = -0.02 \pm 0.04. \tag{7}$$

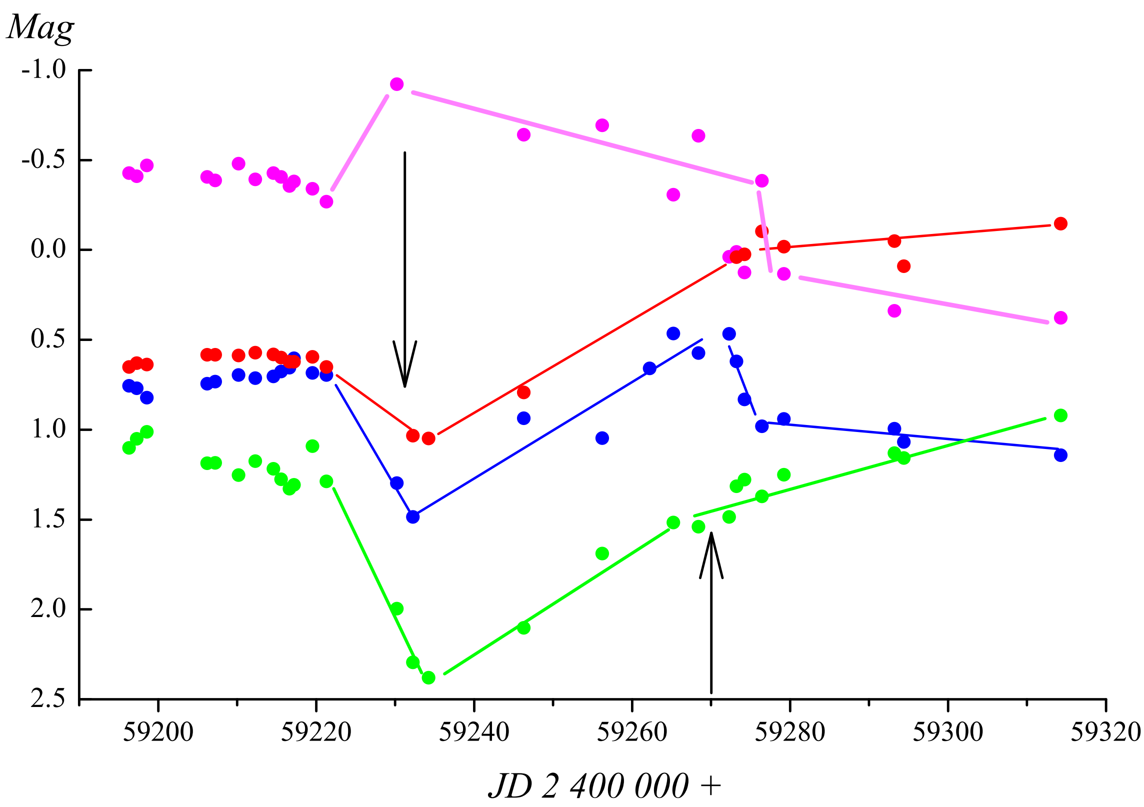

Figure 4.
Evolution of color indices of V1112 Per, $U-B$ - magenta, $B-V$ - blue, $V-Rc$ - green, $Rc-Ic$ - red. The downward pointing arrow indicates dust emission. The upward arrow marks the beginning of the nebular stage. Interestingly, dust absorption in U is less than in B.

The observed color of V1112 Per two magnitudes below maximum is $B-V = 0^{\rm m}.74$, which thus yields $E(B-V) = 0^{\rm m}.76$;

(4) from the relation suggested by Miroshnichenko (1988) who developed the photometric method to determine interstellar extinction towards Novae. He found that during "stability stage", which occurs not very long after maximum, when both $U-B$ and $B-V$ indices do not change systematically, the color excess is given by:

$$E(B-V) = (B-V)_{\rm SS} + 0^{\rm m}.11 \pm 0^{\rm m}.02, \tag{8}$$

where $(B-V)_{\rm SS}$ is the mean color index during the stability stage. For V1112 Per, the stability stage lasted from JD 2,459,190 to JD 2,459,207. For $(B-V)_{\rm SS} = 0^{\rm m}.76$, we find a corresponding $E(B-V) = 0^{\rm m}.87$.

The mean reddening found from the data mentioned above is $E(B-V) = 0^{\rm m}.74 \pm 0^{\rm m}.07$. This value is higher than follows from data in Green et al. (2015) for this region and the distance of 6 kpc or more (piercing the Galaxy's disk through and through), $E(B-V) = 0^{\rm m}.51 \pm 0^{\rm m}.04$. Multicolor photometry of other objects under study, such as V2544 Cyg (Volkov et al. 2017) and V839 Cep (Volkov et al. 2024), has already shown significant excesses of interstellar extinction compared to survey data.

The corresponding absorption in V and B bands is $A_V = 2^{\rm m}.31 \pm 0^{\rm m}.15$ and $A_B = 3^{\rm m}.09 \pm 0^{\rm m}.20$. The resulting distance moduli of V1112 Per are $V_{\rm max} - MV_{\rm max} = 13^{\rm m}.59 \pm 0^{\rm m}.15$ and $B_{\rm max} - MB_{\rm max} = 13^{\rm m}.39 \pm 0^{\rm m}.40$, corresponding to a distance of 5.2 ± 0.4 kpc.

Table 2: U, B, V, Rc, R, Ic, I magnitudes of V1112 Per

JD 2 400 000 +	U	B	V	Rc	R	Ic	I
59196.3199	9.928	10.355	9.600	8.499	–	7.848	–
	0.002	0.001	0.001	0.001	–	0.002	–
59197.2814	9.884	10.295	9.526	8.474	–	7.846	–
	0.007	0.004	0.004	0.002	–	0.002	–
59198.5451	9.830	10.301	9.479	8.467	–	7.831	–
	0.005	0.005	0.004	0.003	–	0.003	–
59206.1970	10.542	10.948	10.203	9.017	–	8.435	–
	0.000	0.009	0.003	0.003	–	0.004	–
59207.2274	10.571	10.957	10.225	9.040	–	8.455	–
	0.016	0.003	0.003	0.002	–	0.003	–
59210.1605	10.665	11.146	10.450	9.197	–	8.610	–
	0.000	0.004	0.003	0.002	–	0.000	–
59212.2962	10.705	11.096	10.383	9.209	–	8.638	–
	0.005	0.003	0.003	0.002	–	0.002	–
59214.5913	10.852	11.279	10.575	9.358	–	8.776	–
	0.005	0.005	0.004	0.003	–	0.003	–
59215.5722	10.965	11.371	10.695	9.420	–	8.822	–
	0.004	0.002	0.003	0.003	–	0.004	–
59216.5966	11.163	11.517	10.862	9.533	–	8.912	–
	0.009	0.004	0.003	0.002	–	0.002	–
59217.1714	11.136	11.518	10.915	9.608	–	8.987	–
	0.003	0.003	0.002	0.001	–	0.001	–
59219.5394	11.132	11.472	10.787	9.695	–	9.101	–
	0.015	0.002	0.002	0.002	–	0.002	–
59221.3016	11.935	12.203	11.507	10.220	–	9.569	–
	0.004	0.002	0.002	0.001	–	0.001	–
59230.1971	14.644	15.567	14.270	12.275	11.702	–	10.266
	0.012	0.011	0.004	0.005	0.002	–	0.002
59232.2420	-	16.388	14.901	12.608	–	11.574	–
	-	0.100	0.050	0.050	–	0.070	–
59234.2201	-	-	15.150	12.770	–	11.720	–
	-	-	0.009	0.003	–	0.004	–
59246.2820	15.949	16.590	15.652	13.549	–	12.756	–
	0.026	0.020	0.020	0.002	–	0.004	–
59256.2049	16.190	16.883	15.837	14.148	13.692	–	12.715
	0.000	0.040	0.008	0.007	0.003	–	0.007
59262.2287	-	16.631	15.972	-	–	–	–
	-	0.050	0.050	-	–	–	–
59265.2024	16.165	16.472	16.008	14.491	14.094	–	13.362
	0.050	0.017	0.009	0.008	0.005	–	0.013
59268.4040	16.026	16.661	16.088	14.548	14.159	–	13.511
	0.210	0.081	0.022	0.015	0.013	–	0.023
59272.2774	16.497	16.459	15.993	14.508	14.133	–	13.591
	0.082	0.024	0.013	0.006	0.007	–	0.008
59273.2132	16.517	16.506	15.737	14.423	–	14.383	–
	0.075	0.024	0.021	0.007	–	0.007	–
59274.2073	16.646	16.521	15.690	14.413	–	14.388	–
	0.034	0.011	0.002	0.005	–	0.007	–
59276.4121	16.339	16.724	15.743	14.373	–	14.477	–
	0.210	0.019	0.054	0.009	–	0.021	–
59279.2216	16.604	16.471	15.531	14.280	–	14.298	–
	0.039	0.009	0.005	0.003	–	0.006	–
59293.2183	16.389	16.051	15.056	13.925	–	13.975	–
	0.105	0.001	0.035	0.006	–	0.010	–
59294.3818	-	16.057	14.988	13.830	–	13.739	–
	-	0.063	0.080	0.021	–	0.100	–
59314.2565	15.870	15.493	14.352	13.432	–	13.578	–
	0.076	0.005	0.005	0.004	–	0.012	–

4 Fast variability

We examined our data for early periodic variability. For this purpose, observations with dates after JD 2 459 230 were corrected for trends and brought to the same level. The periods were searched in the interval from $0\overset{\mathrm{d}}{.}02$ to $5\overset{\mathrm{d}}{.}2$. The algorithm suggested by Volkov (2022) was used. This program is well suited for searching for small-amplitude oscillations of arbitrary shape, it uses the sliding average algorithm. The period $0\overset{\mathrm{d}}{.}054$ produces a small peak on the periodogram in the V photometric band. For the remaining photometric bands, traces of oscillations were not found. This period does not coincide with that suggested by Schmidt (2021), $0\overset{\mathrm{d}}{.}0927$ day. A plot of data phased with our period is presented in Fig. 5.

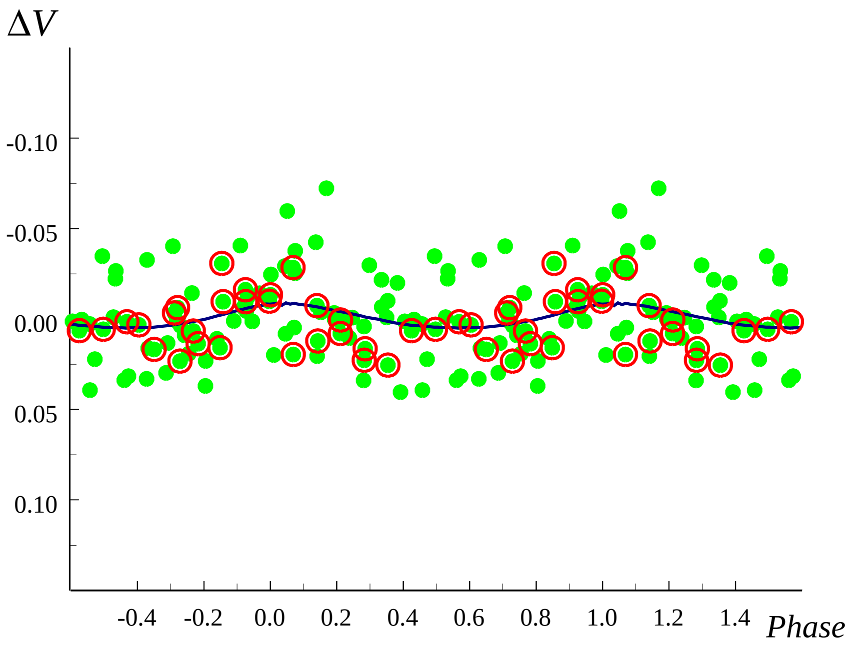

Figure 5.
Our observations after JD 2,459,230 phased with the period $0\overset{\mathrm{d}}{.}054$. Data points circled with red are individual nights 2,459,230 and 2,459,314. The dark sine-shaped curve is for the sliding mean.

Acknowledgements.

This study has made use of the SIMBAD database of the Strasbourg Astronomical Data Center (France).

The study was conducted under the state assignment of Lomonosov Moscow State University.

I would like to express my sincere gratitude to the editor of the journal, Prof. N.N. Samus, for his fruitful discussions of the manuscript and for introducing important editorial improvements.

References:

Chochol, D., Katysheva, N. A., Pribulla, T., Shugarov, S. Yu., Škoda, P., Šlechta, M., & Volkov, I. M. 2005a, *ASP Conference Series*, eds. J.-M. Hameury & J.-P. Lasota, **330**, 439

Chochol, D, Katysheva, N. A., Pribulla, T., Schmidtobreick, L., Shugarov, S. Yu., Škoda, P., Šlechta, M., Vittone, A. A., & Volkov, I. M. 2005b, *Contrib. Astron. Obs. Skalnaté Pleso*, **35**, No. 2, 107

Chochol, D, Katysheva, N. A., Shugarov, S. Yu., & Volkov, I. M. 2009, *Contrib. Astron. Obs. Skalnaté Pleso*, **39**, No. 1, 43

Chochol, D., Katysheva, N. A., Shugarov, S. Yu., Volkov, I. M., & Andreev, M. V. 2010, *Contrib. Astron. Obs. Skalnaté Pleso*, **40**, No. 1, 19

Chochol, D, Shugarov, S., Pribulla, T., & Volkov, I. 2014, *Contrib. Astron. Obs. Skalnaté Pleso*, **43**, No. 3, 330

Chochol, D., Hambalek, L., Komzik, R., et al. 2020, *The Astronomer's Telegram*, No. 14243

Della Valle, M. & Livio, M. 1995, *Astrophys. J.*, **452**, No. 2, 704

Downes, R. A. & Duerbeck, H. W. 2000, *Astron. J.*, **120**, No. 4, 2007

Green, G. M., Schlafly, E. F., Finkbeiner, D. P., et al. 2015, *Astrophys. J.*, **810**, No. 1, article id. 25

Hachisu, I. and Kato, M., 2014, *ApJ*, **785**, No. 2, article id. 97

Katysheva, N., Shugarov, S., Chochol, D., Pavlenko, E., Volkov, I., et al. 2013, *Central European Astrophys. Bulletin*, **37**, 335

Landolt, A. U. 2009, *Astron. J.*, **137**, No. 5, 4186

Livio, M. 1992, *Astrophys. J.*, **393**, No. 2, 516

Mermilliod, J. C., Mermilliod, M., & Hauck, B. 1997, *Astron. & Astrophys., Suppl. Ser.*, **124**, 349

Miroshnichenko, A. C. 1988, *Soviet Astronomy*, **32**, No. 3, 298

Munari, U., Castellani, F., Dallaporta, S., & Andreoli, V., 2020, *The Astronomer's Telegram*, No. 14224

Nikolenko, I. V., Kryuchkov, S. V., Barabanov, S. I., & Volkov, I. M. 2019, *Nauch. Tr. Inst. Astron. RAN*, **4**, 85

Pfau, W. 1976, *Astron. & Astrophys.*, **50**, No. 1, 113

Schmidt, R. E. 2021, *Journal of the AAVSO*, **49**, No. 1. 99

Taylor, B. J. 1986, *Astrophys. J., Suppl. Ser.*, **60**, No. 2, 577

van den Bergh, S., & Younger, P.F̃. 1987, *Astron. & Astrophys., Suppl. Ser.*, **70**, No. 1, 125

Volkov, I. M. 2022, *Peremennye Zvezdy / Variable Stars*, **42**, No. 1, 1

Volkov, I., Bagaev, L., & Chochol, D. 2017, *Proceedings of the ESO Workshop on the Impact of Binaries on Stellar Evolution, ESO Garching, July 3-7, 2017.* https://istina.msu.ru/conferences/presentations/64686337/

Volkov, I. M., Volkova, A. S., & Bagaev, L. A. 2024, *Astron. Rep.*, **68**, No. 9, 886